Evaluation of Structural Integrity under Bursting Conditions of Heat Treated 2219 Al-Alloy Pipes Using Finite Element Analysis

M. Akhil[1], A. Chennakesava Reddy[2]

[1]UG student, Department of Mechanical Engineering, JNTUH College of Engineering, Hyderabad, India
[2]Professor, Department of Mechanical Engineering, JNTUH College of Engineering, Hyderabad, India

Abstract: ***The structural integrity of liquid and gas pipe lines is very important with respect safety. In this paper 3D finite element analysis and Taguchi technique were employed to investigate fracture criteria of AA2219 Al-alloy pipes subjected to internal bursting pressure. The ultimate tensile strength criterion was employed to study the failure of pipes. The pipe thickness, crack length and heat treatment were the major dominating control factors affecting the bursting of pipes.***

Keywords: AA2219 Al-alloy, bursting pressure, crack length, crack depth, heat treatment, finite element analysis

1. Introduction

Pipeline flaws resulting from degradation of the protective coating or cathodic protection degradation, a corrosive environment, or third party damage may lead to corrosion, crack or hybrid crack-in-corrosion flaws. Aluminum alloys have high corrosion resistance. The strength of these alloys can be reduced when they are subjected to temperatures of about 200 to 250°C. However, their strength can be increased at subzero temperatures. Numerous methods have been developed for predicting the burst pressure of blunt part-wall defects, which characterize the behavior of typical corrosion defects [1, 2, 3, 4]. ASME B31G, DNV-RP-F101, SHELL-92 and RESTRENG were applied to assess the strength of thin tubes [5, 6, 7, 8]. The finite element analysis (FEA) is one of the most efficient tools to quantify reliably the remaining strength of corroded pipes. Elastic-Plastic finite element models have been used to provide more accurate results in evaluating the corrosion defects [9, 10, 11].

The objectives of the present work were to evaluate the structural integrity of heat treated AA2219 Al-alloy pipes with different crack dimensions subjected to bursting pressure using finite element analysis and Taguchi techniques.

Table 1: Control factors and their levels

Factor	*Symbol*	*Level–1*	*Level–2*	*Level–3*
Thickness, mm	A	1.0	1.2	1.5
Length of crack, mm	B	25	50	75
Depth of crack	C	30%t	40%t	50%t
Heat treatment	D	T3	T81	T87

where t is pipe thickness

2. Materials and Methods

The material of pipes was AA2219 Al-alloy. The chosen control parameters are summarized in table 1. The control factors were assigned to the various columns of orthogonal array (OA), L9 as given in table 2. The pipe model and surface crack were modeled using computer aided design tools [12]. A surface notch made on the outer surface of the pipe specimen. The dimensions of notch are given in figure 1.

Table 2: Orthogonal Array (L9) and control factors

Treat No.	*A*	*B*	*C*	*D*
1	1	1	1	1
2	1	2	2	2
3	1	3	3	3
4	2	1	2	3
5	2	2	3	1
6	2	3	1	2
7	3	1	3	2
8	3	2	1	3
9	3	3	2	1

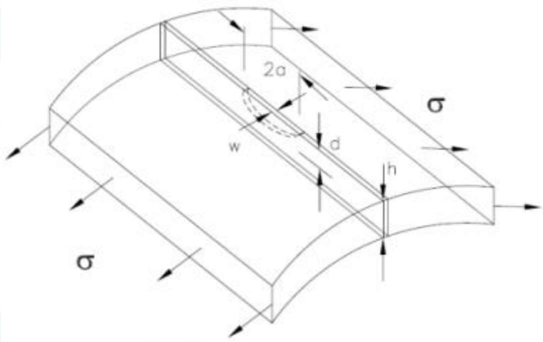

Figure 1: The Crack dimensions.

The operating pressure was obtained from the following expression:

$$P = 0.60\,\sigma_y(2t/D) \times (1 - t/d) \quad (1)$$

where P is the design pressure (MPa), σ_y is the yield strength (MPa), t is the nominal wall thickness (mm), D is the nominal outside diameter (mm), and d is the crack depth.

The ANSYS code was used to estimate the stresses induced in the pipes under applied pressure for predefined crack dimensions and type of heat treatment. The pipe was meshed with tetrahedron elements [13]. A three-dimensional semi-elliptical crack was initiated on the pipe surface. The crack was oriented with respect to pipe axis as shown in figure 2. The pressure obtained from Eq. (1) was applied on the inner surface of pipe.

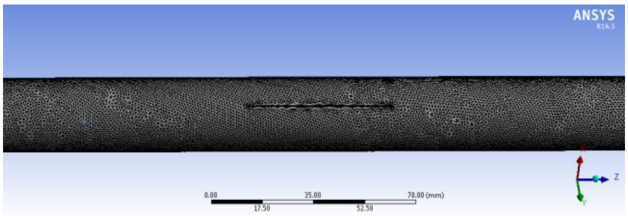

Figure 2: Meshing of crack and pipe.

If the failure is defined by material ultimate tensile strength, it follows that the design goal is to limit the maximum equivalent stress to be less than the ultimate tensile strength of the material:

$$ES/UTS < 1 \quad (2)$$

where, ES is the equivalent stress and UTS is the yield strength of AA2219 Al-alloy.

3. Results and Discussion

The finite element analysis was carried out twice with two element sizes of 1.0 mm and 1.5 mm density according Taguchi design of experimentation.

3.1 Static deformation

The total deformations of analyzed pipes are shown in figure 3. For the pipes having thickness of 1mm the maximum total deformation of 0.039 mm was observed with test coupon 3 and the minimum total deformation of 0.0186 mm test coupon 1. For the pipes having thickness of 1.2 mm the maximum total deformation of 0.0322 mm was observed with test coupon 4 and the minimum total deformation of 0.0221 mm test coupon 6. For the pipes having thickness of 1.5 mm the maximum total deformation of 0.0296 mm was observed with test coupon 8 and the minimum total deformation of 0.0209 mm test coupon 9.

3.2 Equivalent stress distribution across the crack

The equivalent stress distribution across the crack for all the pipes is shown in figure 4. The maximum equivalent stress of test coupons 1, 2, 3, 4, 5, 6, 7, 8 and 9, respectively 386.98 MPa, 471.59 MPa, 1195.50 MPa, 656.72 MPa, 365.32 MPa, 558.61 MPa, 460.70 MPa, 608.65 and 475.77 MPa. The equivalent stresses of the pipes 1, 5 and 9 were belonging to heat treatment, T3. For the pipe 5 only the equivalent stress was not surpassed the ultimate tensile strength (369 MPa) of AA2219 Al-alloy. The equivalent stresses of the pipes 2, 6 and 7 were belonging to heat treatment, T4. For the entire pipes the equivalent stress went beyond the ultimate tensile strength (400 MPa) of AA2219 Al-alloy. The equivalent stresses of trials 3, 4 and 8 were belonging to heat treatment, T6. For all pipes the equivalent stress was exceeded the ultimate tensile strength (476 MPa) of AA2219 Al-alloy.

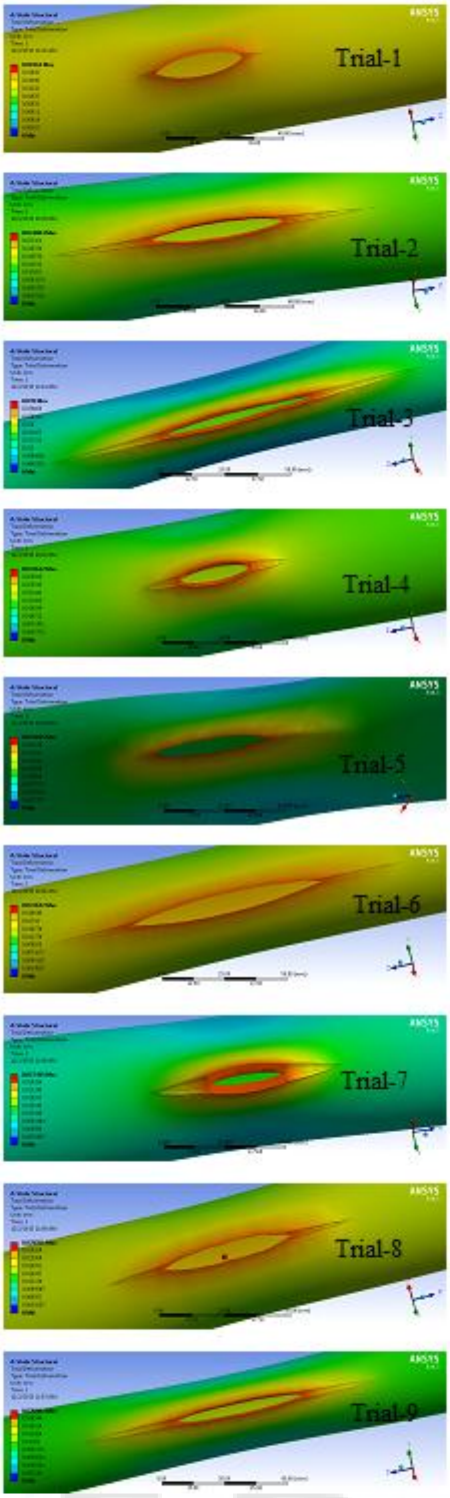

Figure 3: Total deformations of all test coupons.

3.3 J-integral

The path dependence of the J-integral is displayed for all nine pipes in figure 5. The maximum values of J-integral were 0.748, 0.757 and 0.673 MJ/mm^2 with the pies 3, 4 and 7 respectively having the displacements of 0.039, 0.032 and 0.0275 mm. The minimum value of J-integral was 0.220 MJ/mm^2 with the test coupon 1 having the displacement of 0.0186 mm. Therefore, the J-integral is directly proportional to the displacement of the load applied on the pipe. The path dependence of the J-integral was much more significant in a large deformation analysis [14].

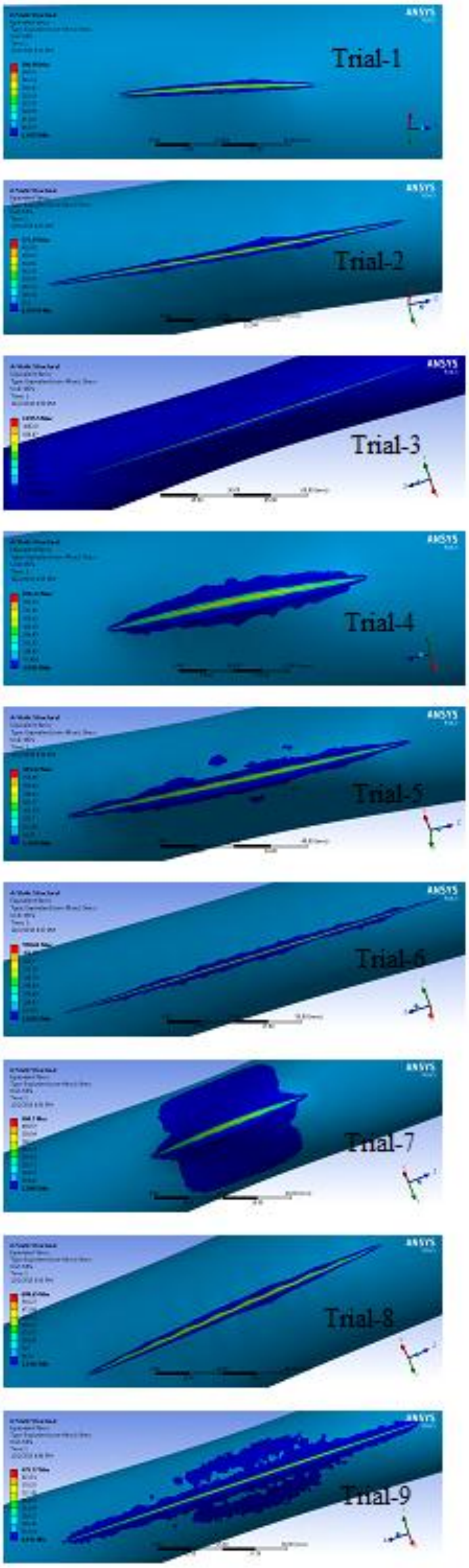

Figure 4: Equivalent stresses of all test coupons.

3.4 Stress Intensity Factors

Figure 6 shows the variations of stress intensity factor, KI along the initial crack-front for all pipes. The KI had the maximum values of 247.38, 248.95 and 233.97 MPa-sqrt(mm) respectively for the pipes 3, 4 and 7. The stress intensity factors, KII and KIII were found insignificant.

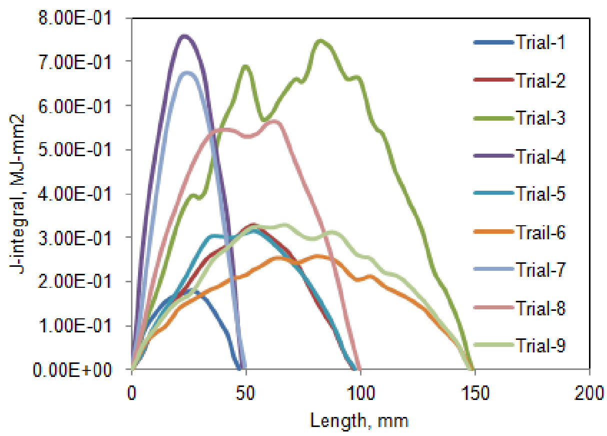

Figure 5: J-Integral values of all test coupons.

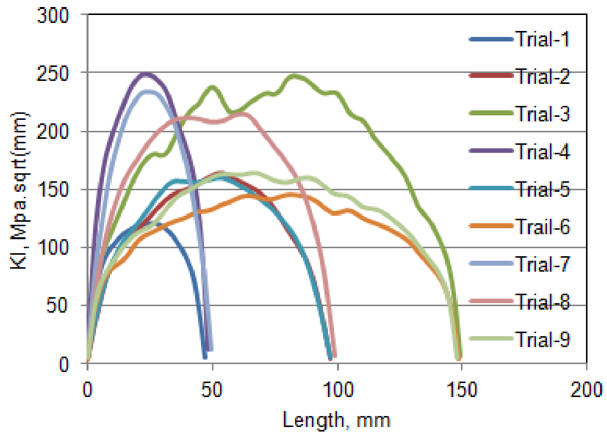

Figure 6: Stress intensity factors, KI of all test coupons.

3.5 Failure Criteria

The ANOVA summary of ultimate tensile strength (UTS) failure criterion is given in table 3. All parameters were accepted at 90% confidence level. The percent contribution indicates that the pipe thickness, crack length and the heat treatment of the pipes had, respectively, contributed 14.27%, 38.58% and 37.67% in the total variation for the UTS criterion. The influences of crack depth (C) were low.

Table 3: ANOVA summary of the UTS failure criteria

Source	*Sum 1*	*Sum 2*	*Sum 3*	*SS*	*v*	*V*	*F*	*P*
A	9.53	7.45	7.51	0.47	2	0.235	1704.26	14.27
B	7.24	6.85	10.40	1.27	2	0.635	4605.14	38.58
C	7.47	7.76	9.26	0.31	2	0.155	1124.09	9.41
D	6.74	9.12	24.49	1.24	2	0.62	4496.36	37.67
Error				0.00124	9	0.00014	1.00	0.07
T	30.98	31.18	51.67	3.29124	17			100

The effect of pipe thickness on the failure criteria is shown in figure 7. The failure of the pipes decreased with the increase of pipe thickness. The failure of pipes was high at crack length of 75 mm. The failure of pipes having crack lengths of 25 mm and 50 mm was not much invariant (figure 8). The failure was minimal for the pipes undergone the heat treatment T3 (figure 9). The optimum conditions of test coupon 5 would satisfy the failure criterion (ES/UTS = 0.99 <1.0) while all other conditions were failed to satisfy the failure criterion.

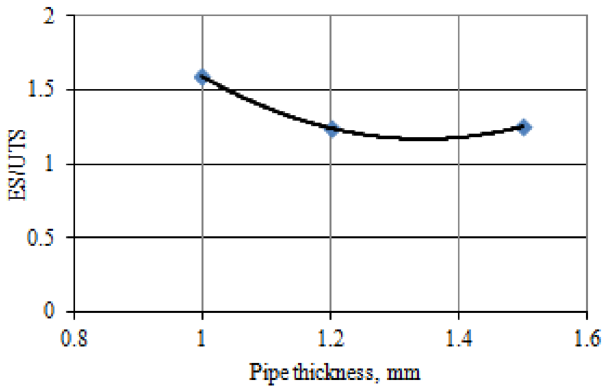

Figure 7: Effect of pipe thickness on the failure criterion.

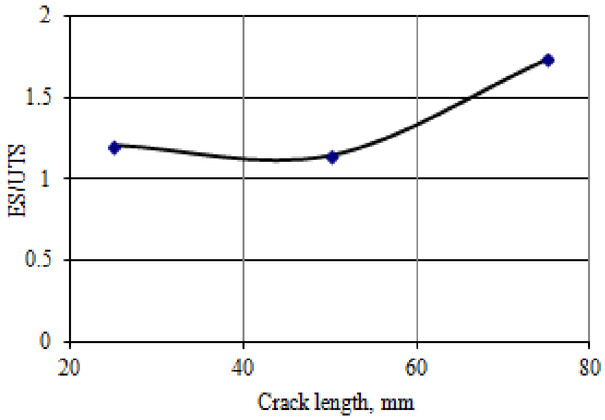

Figure 8: Effect of crack length on the failure criterion.

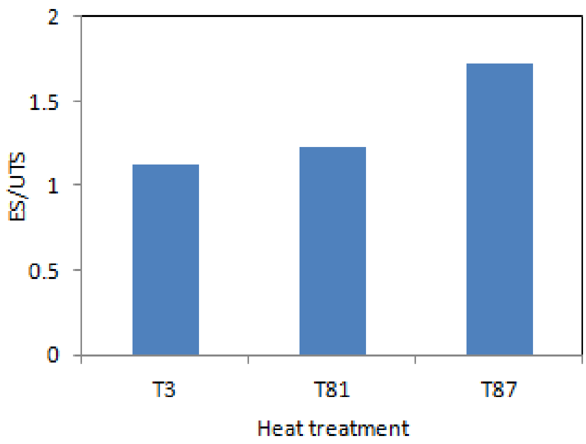

Figure 9: Effect of heat treatment on the failure criterion.

4. Conclusions

The failure of pipes increases with the increase of crack length. As the pipe thickness increases the failure of the pipes decreases. The failure of pipes under bursting pressure was low for the pipes heat treated with T3 conditions because of low hardness as compared to T81 and T87 heat treatments.

References

[1] American National Standards Institute (ANSI) / American Society of Mechanical Engineers (ASME): Manual for determining the remaining strength of corroded pipelines, ASME B31G, 1991.

[2] ANON; DNV-RP-F101, Corroded Pipelines, Det Norske Veritas, 1999.

[3] RITCHIE,D., LAST,S.; Burst Criteria of Corroded Pipelines - Defect Acceptance Criteria, Paper 32, Proceedings of the EPRG/PRC 10th Biennial Joint Technical Meeting on Line Pipe Research, Cambridge, UK, 18-21 April 1995, pp. 32-1 - 32-11.

[4] PRCI-Documents L51688B, A Modified Criterion for Evaluating the Remaining Strength of Corroded Pipe, 1989.

[5] A. Chennakesava Reddy, Evaluation of bursting pressure of thin walled 316 stainless steel tubes based on ASME B31G criterion, National Conference on Advances in Design Approaches and Production Technologies (ADAPT-2005), 22-23rd August 2005, Hyderabad, pp.225-228.

[6] A. Chennakesava Reddy, Evaluation of bursting pressure of thin walled 304 stainless steel tubes based on DNV RP

F101criterion, National Conference on Advances in Design Approaches and Production Technologies (ADAPT-2005), 22-23rd August 2005, Hyderabad, pp.229-231.
[7] Chennakesava Reddy, Reliability assessment of corrosion in cold rolled 302 stainless steel tubes based on SHELL-92 criterion, National Conference on Advances in Design Approaches and Production Technologies (ADAPT-2005), 22-23rd August 2005, Hyderabad, pp.232-234.
[8] A. Chennakesava Reddy, Reliability assessment of corrosion in cold rolled 305 stainless steel tubes based on RSTRENG criterion, National Conference on Advances in Design Approaches and Production Technologies (ADAPT-2005), 22-23rd August 2005, Hyderabad, pp.235-237.
[9] D.U.M. Manikanta, A. Chennakesava Reddy, "Fracture Behavior of 6061 Al-Alloy Pipes under Bursting Loads with Crack Depth Variation," International Journal of Scientific & Engineering Research, Vol. 6, 338-343, 2015.
[10] D.U.M. Manikanta, A. Chennakesava Reddy, "Fracture Behavior of 6061 Al-Alloy Pipes under Bursting Loads with Crack Length Variation," International Journal of Advanced Research, ISSN: 2320-5407, Vol. 3, No. 4, pp. 657-665, 2015.
[11] D.U.M. Manikanta, A. Chennakesava Reddy, "Optimization of Fracture Behavior of AA6061 Al- Alloy Pipes Using Finite Element Analysis," International Journal of Science and Research, Vol. 4, pp. 1509-1515, 2015.
[12] C.R. Alavala, "CAD/CAM: Concepts and Applications," PHI Learning Pvt. Ltd., New Delhi, 2008.
[13] C.R. Alavala, "Finite element methods: Basic concepts and applications," PHI Learning Pvt. Ltd., New Delhi, 2008.
[14] J. Newman, I.S. Raju, "An Empirical Stress-Intensity Factor Equation for the Surface Crack," Engineering Fracture Mechanics vol.15, pp.185–192, 1981